Physics Scholarship   Physics

MeV magnetosheath ions energized at the bow shock

S. Chang

J. D. Scudder

K. Kudela

Harlan E. Spence
Boston University, harlan.spence@unh.edu

J. F. Fennell

See next page for additional authors

Recommended Citation

Chang, S.-W., J. D. Scudder, K. Kudela, H. E. Spence, J. F. Fennell, R. P. Lepping, R. P. Lin, and C. T. Russell (2001), MeV magnetosheath ions energized at the bow shock, J. Geophys. Res.,106(A9), 19101–19115, doi:10.1029/2000JA003037.

Authors

S. Chang, J. D. Scudder, K. Kudela, Harlan E. Spence, J. F. Fennell, R. P. Lepping, R. P. Lin, and C. T. Russell

MeV magnetosheath ions energized at the bow shock

S.-W. Chang,[1,2] J. D. Scudder,[1] K. Kudela,[3] H. E. Spence,[4]
J. F. Fennell,[5] R. P. Lepping,[6] R. P. Lin,[7] and C. T. Russell[8]

Abstract. A causal relationship between midlatitude magnetosheath energetic ions and bow shock magnetic geometry was previously established for ion energy up to 200 keV e^{-1} for the May 4, 1998, storm event. This study demonstrates that magnetosheath ions with energies above 200 keV up to 1 MeV simply extend the ion spectrum to form a power law tail. Results of cross-correlation analysis suggest that these ions also come directly from the quasi-parallel bow shock, not the magnetosphere. This is confirmed by a comparison of energetic ion fluxes simultaneously measured in the magnetosheath and at the quasi-parallel bow shock when both regions are likely connected by the magnetic field lines. We suggest that ions are accelerated at the quasi-parallel bow shock to energies as high as 1 MeV and subsequently transported into the magnetosheath during this event.

1. Introduction

Energetic ions of solar wind origin with energies up to ~1 MeV are frequently observed in the polar cusp region. It was hypothesized that local acceleration in the cusp is responsible for these cusp energetic particles (CEPs) [e.g., *Chen et al.*, 1998]. This view was challenged by *Chang et al.* [1998], who showed that cusp energetic ion spectra (< 300 keV e^{-1}) matched very well with a large body of bow shock ion spectra. *Chang et al.* [1998] proposed that solar wind ions are accelerated at the quasi-parallel bow shock and subsequently transported into the cusp along interconnected magnetic field lines. Within this framework, bow shock accelerated ions should appear in the midlatitude dayside magnetosheath upstream from the cusp.

This prediction has been confirmed in a recent study of energetic ions observed by Polar at the above mag-

netosheath region during the May 4, 1998, magnetic storm event [*Chang et al.*, 2000]. In this event, magnetosheath energetic ion fluxes of solar wind origin showed variations as large as 2 orders of magnitude. As expected in the bow shock model, these ion fluxes were anticorrelated with the interplanetary magnetic field (IMF) cone angle at the shock. On the other hand, He$^+$ fluxes presumably of ionospheric origin were quite steady throughout the magnetosheath interval and were not correlated with the cone angle. These results suggest that magnetosheath energetic ions of solar wind origin are extracted from the diffuse ions at the quasi-parallel bow shock [e.g., *Ipavich et al.*, 1981] and that those of ionospheric origin most likely result from the magnetospheric leakage [e.g., *Sibeck et al.*, 1987], consistent with early findings at the low-latitude magnetosheath [e.g., *Fuselier et al.*, 1991].

Delcourt and Sauvaud [1999] show that magnetospheric energetic particles of a few hundreds of keV can leak from the equatorial trapping region at the dayside plasma sheet into the cusp; this injection is favored during substorms. These particles may further escape into the magnetosheath along reconnected magnetic field lines [e.g., *Speiser et al.*, 1981; *Scholer et al.*, 1981]. General views of the source of magnetosheath energetic ions remain the upstream diffuse ions [e.g., *Gosling et al.*, 1978; *Bonifazi and Moreno*, 1981; *Fuselier et al.*, 1991] and magnetospheric leakage near the equatorial magnetopause [e.g., *Sarris et al.*, 1976; *Croley et al.*, 1986; *Sibeck et al.*, 1987].

In this paper we continue the work of *Chang et al.* [2000] (hereinafter referred to as paper 1) on the May 4 storm event, and we perform a similar cross-correlation analysis for ions with energies from 200 keV to 1 MeV, beyond the ion energies in the previous work. Energetic ion fluxes are compared in the solar wind (Wind), quasi-parallel bow shock (Interball-Tail), and midlati-

[1]Department of Physics and Astronomy, University of Iowa, Iowa City, Iowa.

[2]Now at Center for Space Plasma and Aeronomic Research, University of Alabama in Huntsville.

[3]Institute of Experimental Physics, Kosice, Slovakia.

[4]Center for Space Physics, Boston University, Boston, Massachusetts.

[5]The Aerospace Corporation, Los Angeles, California.

[6]NASA Goddard Space Flight Center, Greenbelt, Maryland.

[7]Space Sciences Laboratory, University of California, Berkeley, California.

[8]Institute of Geophysics and Planetary Physics, University of California, Los Angeles, California.

tude magnetosheath (Polar). In this way, concurrent measurements of energetic ions in the magnetosheath and the bow shock source regions are provided for the first time in the literature. Our analysis indicates that ions were accelerated up to an energy as high as 1 MeV at the shock and subsequently transported into the magnetosheath. This result is in direct contradiction with the claim by *Chen and Fritz* [1999] that solar wind ions are locally accelerated to MeV in the cusp and then escape into the magnetosheath during this event. Results of ion flux comparison in the magnetosheath and at the bow shock confirm our view of a bow shock source of magnetosheath energetic ions [*Chang et al.*, 2000]. These results then further support our bow shock model of CEPs [*Chang et al.*, 1998].

2. Observations

In addition to the data sets used in paper 1, namely, ion data from Polar/Hydra [*Scudder et al.*, 1995], the Charge and Mass Magnetospheric Ion Composition Ex-

periment (CAMMICE) (refer to *Wilken et al.* [1992] for the Magnetospheric Ion Composition Sensor (MICS) detector), magnetic field data from the Magnetic Field Experiment (MFE) [*Russell et al.*, 1995], IMF data from the Magnetic Field Investigation (MFI) [*Lepping et al.*, 1995], and solar wind data from the Solar Wind Experiment (SWE) [*Ogilvie et al.*, 1995] both on board the Wind spacecraft, we include energetic ions up to 1 MeV observed upstream in the solar wind, bow shock, and magnetosheath in this work. Energetic ions in the solar wind are measured by two detectors of the 3-D Plasma and Energetic Particle Instrument (3DP) [*Lin et al.*, 1995] on board Wind, the ion electrostatic analyzer (PESA-H) ($\sim$5-28 keV) and the semiconductor detector telescopes (SST) open detector ($\sim$71-1017 keV). Energetic ions in the upstream region of bow shock are acquired with the 1p detector of the DOK-2 instrument on Interball-Tail [*Lutsenko et al.*, 1995; *Kudela et al.*, 1995]. The detector covers an energy range from $\sim$21 to 821 keV in 57 logarithmic steps. However, only the energy channels without the background interfer-
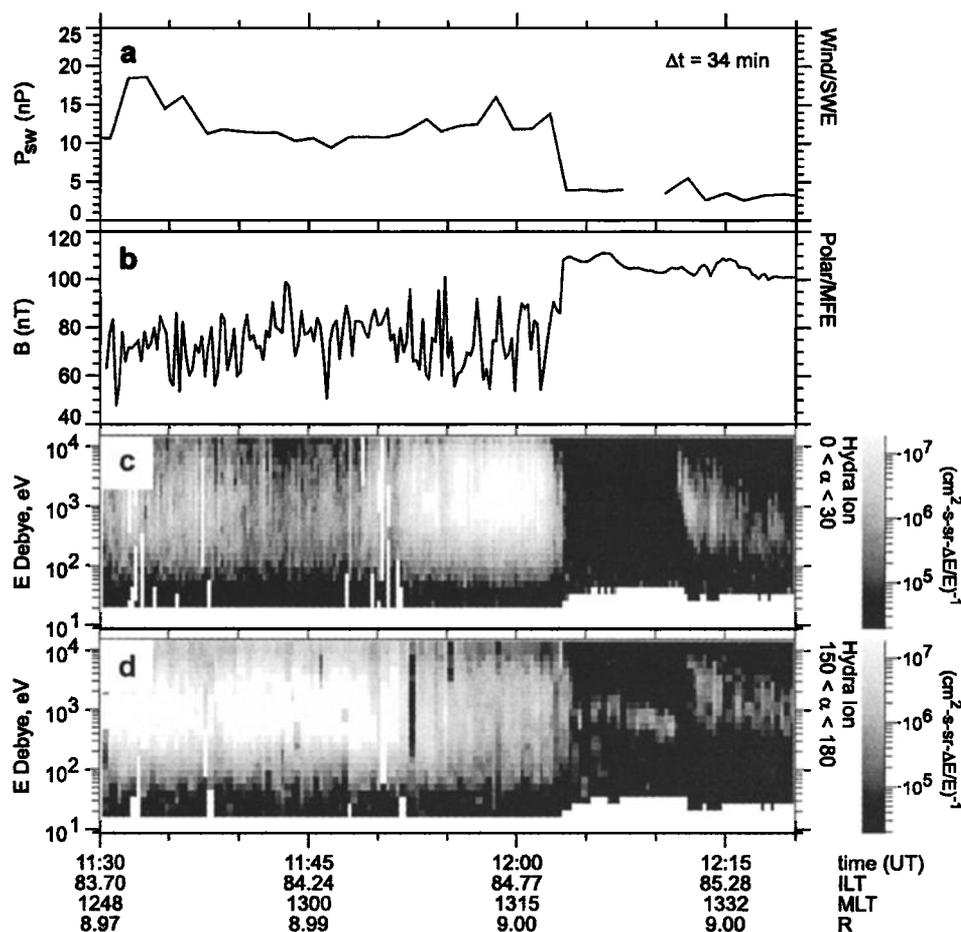
Figure 1. (a) Solar wind dynamic pressure from Wind/SWE, (b) magnetic field magnitude from Polar/MFE, (c) Hydra ion energy-time spectrogram showing ion differential energy flux parallel to B, and (d) Hydra ion energy-time spectrogram showing ion differential energy flux antiparallel to B, from 1120 to 1220 UT on May 4, 1998. Two colors in the spectrogram that are not present in the scale indicate data gaps (white) and ion fluxes above the maximum value in the scale (the brightest gray).

ence are selected for this study (~35-620 keV). In the magnetosheath the Imaging Proton Sensor (IPS) of the Comprehensive Energetic Particle and Pitch Angle Distribution (CEPPAD) measures ion energy from ~14 to 1500 keV for a nearly full angular coverage [*Blake et al.*, 1995]. For the purpose of constructing a full energy spectrum for magnetosheath ions, data used in this study are only extracted from the 90° sensor head whose look direction is perpendicular to the Polar's spin axis to match those of CAMMICE and selected Hydra detectors. Data sampled within the sectors that contain the reflected earthlight are excluded. All the ion data presented in this paper are total ion measurements assuming H^+ response unless specified otherwise for some channels of the CAMMICE instrument.

2.1. Magnetosheath Ion Spectrum

It had been identified in paper 1 from the Hydra ion and electron density, temperature, and bulk flow data and electron angular distribution and MFE magnetic field data, that the Polar spacecraft traversed the midlatitude dayside magnetosheath region for more than 3 hours (~0840-1200 UT) during the May 4, 1998, storm event. As an example, Figure 1 shows solar wind dynamic pressure from Wind/SWE and Polar/MFE magnetic field and Hydra ion data from 1120 to 1220 UT. The solar wind dynamic pressure is lagged by 34 min to align the discontinuity at ~1203 UT in Figure 1a-1d. This lag is nearly identical to our previously estimated solar wind and shocked solar wind propagation time (33 min in Figure 5 of paper 1). Before 1203 UT, Polar was in the magnetosheath as the magnetopause was compressed by the large dynamic pressure. MFE magnetometer detected weak magnetic (**B**) fields and large-amplitude low-frequency waves ($\delta B \sim B$). Hydra detectors measured highly skewed ion fluxes, toward $-\mathbf{B}$ before 1153 UT and $+\mathbf{B}$ after. This reversal occurred as the x and z components of **B** changed sign. As expected, these magnetosheath ions show a strong tailward flow. After the dynamic pressure reduced at 1203 UT, Polar crossed the magnetopause and entered a magnetospheric region on lobe field lines. This is suggested by the simultaneous measurements of large, steady **B** field from MFE and imperceptible ion precipitation and weak ion outflows from Hydra. Later, at 1212 UT, Polar entered the plasma mantle, detecting ion precipitation with the typical characteristic of the energy-latitude dispersion [e.g., *Reiff et al.*, 1977].

The magnetosheath ion distribution is highly skewed in the spacecraft frame because of the flow. As demonstrated in Figure 2, the ion distribution function antiparallel to **B** consists of a Maxwellian thermal component and a suprathermal tail. The peak of the distribution function appears at ~390 km s^{-1}. In contrast, ion distribution function parallel to **B** is ~2 orders of magnitude smaller than the antiparallel one. Both distributions roughly mirror each other about the ion veloc-
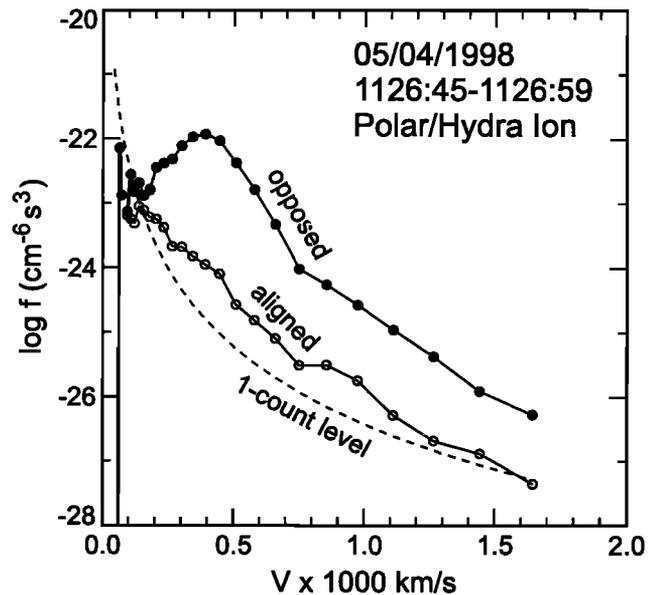
Figure 2. Magnetosheath ion distribution function observed by Hydra for two pitch angle ranges; thick line is for 150°-180°, and thin line is for 0°-30°.

ity at the peak distribution, reflecting a superposition of a flowing Maxwellian and a suprathermal tail distribution as it would be expected for the undisturbed magnetosheath plasmas. Therefore ion distribution is symmetric in the first approximation in the rest frame of plasmas. This type of distribution is persistently observed throughout the magnetosheath intervals within 0840-1200 UT.

Figure 3 depicts the average ion spectrum in the magnetosheath intervals within 0842-1158 UT from Hydra, CAMMICE, and CEPPAD. The Hydra and CAMMICE spectra are reproduced from Figure 6 of paper 1. Data from these instruments presented here are well calibrated for this event as demonstrated by the good matches among the individual spectral curves. The composite spectrum is continuous with a spectral break occurring at ~40 keV. The spectral shape for the CAMMICE energetic ions from ~40 to 200 keV is best described by a Maxwellian or exponential function. As shown by the good agreement between the curve and data points in Figure 3 for ions within this energy range, the latter function yields an excellent fit. However, CEPPAD ions with energies above ~200 keV do not agree with this fit. They simply extend the CAMMICE spectrum to form an energy power law tail with a spectral index of 3.9, illustrated by the straight line fitting the last six data points. The spectral shape of energetic ions becomes obvious when their spectrum is presented in the formats in Figure 4. From left to right, the straight lines represent a Maxwellian, exponential (both covering ~40-200 keV), and power law distribution (~200-1000 keV), respectively. These results indicate that the energetic tail of magnetosheath ion spectrum from ~40 keV to 1 MeV is best described by a
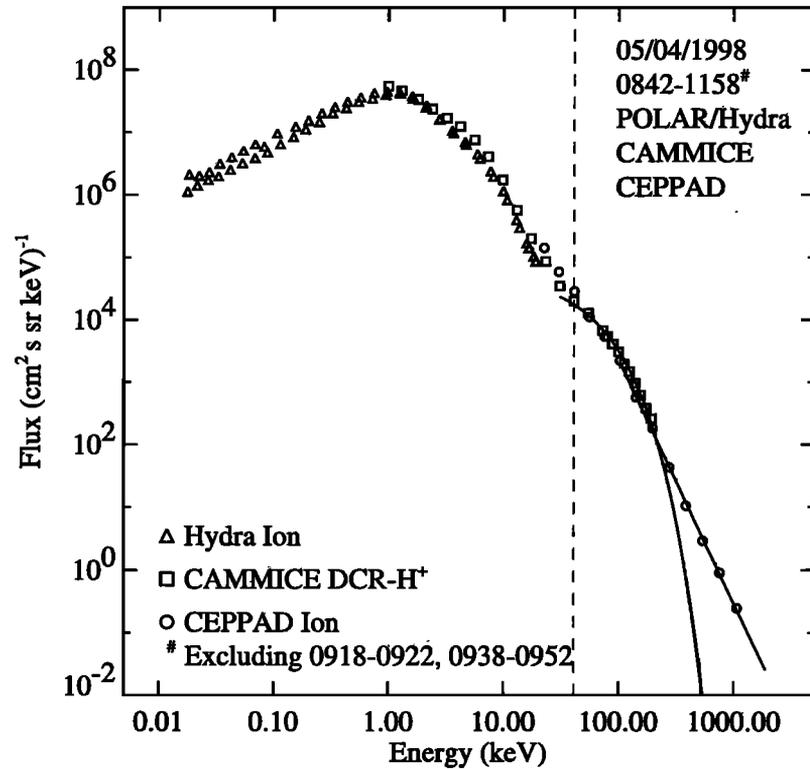
Figure 3. Energy spectrum of magnetosheath ions from Polar/Hydra, CAMMICE, and CEP-PAD averaged over the interval 0842-1158 UT excluding the solar wind intervals on May 4, 1998. The composite spectrum is continuous with a spectral break at ~40 keV (vertical dashed line). CAMMICE ions from ~40 to 200 keV are fitted by an exponential function, and CEPPAD ions from ~200 keV to 1 MeV are fitted by a power law.
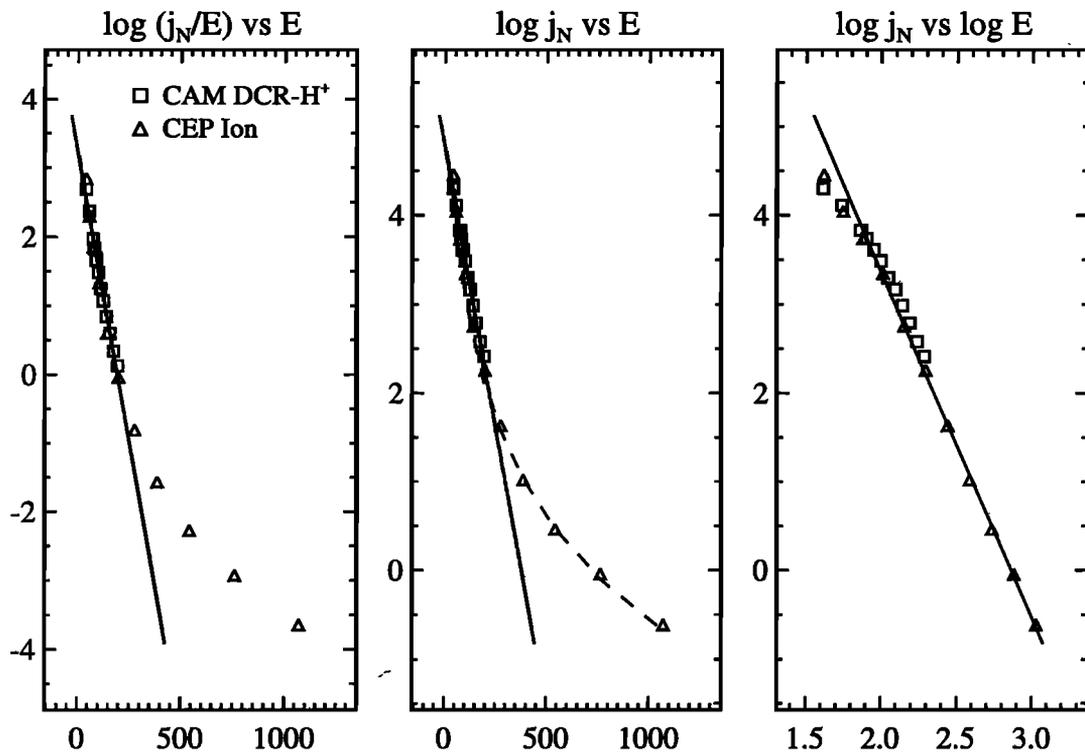
Figure 4. Energy spectrum of magnetosheath energetic ions (~40-1000 keV) extracted from Figure 3. Lower-energy ions (~40-200 keV) can be fitted by a Maxwellian (left) or an exponential function (middle) and higher-energy ions (~200-1000 keV) are fitted by a power law (right), where j_N in $(cm^2 \, s \, sr \, keV)^{-1}$ and E in keV. The dashed curve in the middle panel represents a κ distribution with $\kappa = 4$.
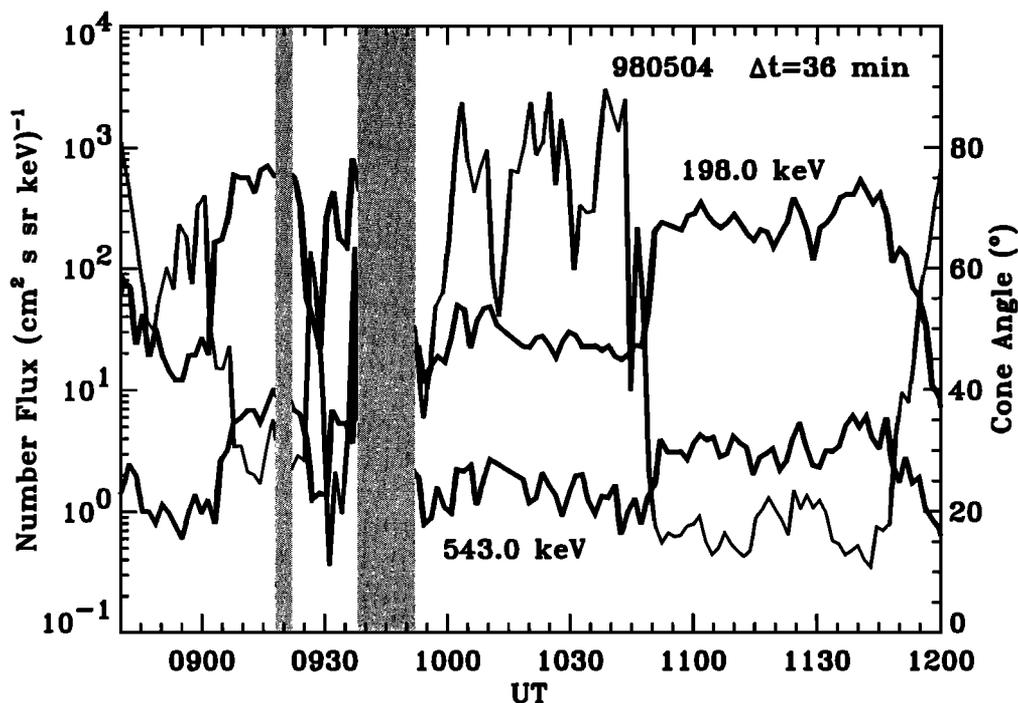
Figure 5. CEPPAD ion fluxes at two energy channels (thick lines, 198 keV above and 540 keV below), during 0840-1200 UT and θ_{Bx} (thin line) from Wind/MFI lagged by 36 min. Ion fluxes at both energies show similar temporal variations and are anticorrelated with θ_{Bx}.

κ distribution [*Vasyliunas*, 1968], as shown in the middle panel of Figure 4 by the dashed curve with $\kappa = 4$. Ions within this energy range plausibly come from one source region.

2.2. Cross-Correlation Analysis

Figure 5 presents CEPPAD ion differential number fluxes measured at two energy channels, 198.0 and 543.0 keV, during the magnetosheath intervals within 0840-1200 UT. Both channels show similar temporal variations which can be as large as 2 orders of magnitude. An opposite variation appears in the IMF cone angle θ_{Bx} from Wind/MFI when it is lagged by 36 min as illustrated by the thin curve. This suggests that ion fluxes at both energy channels are anticorrelated with θ_{Bx}. As we noted in paper 1, θ_{Bx} used here for the cross-correlation analysis serves as a proxy for the actual θ_{Bn} that positions Polar in the foreshock geometry.

A cross-correlation analysis was performed between each of the above two flux profiles and the θ_{Bx} measured at the Wind spacecraft assuming a lag ranging from 0 to 60 min with an increment of 1 min. Results are given in Figure 6. Both correlation curves are very similar. They both demonstrate a trend that correlation coefficient monotonically decreases toward the peak as the assumed time lag increases from 0 toward 36 min and then monotonically increases toward 0 as the lag increases toward 60 min. The peak correlation coefficient and the corresponding lag are (−0.67, 34 min) and (−0.62, 37 min) for 198 and 543 keV ions, respectively. These features of unique peak correlation at a lag of ~35 min are quite consistent with the results from our

previous analysis of the CAMMICE energetic ions (40-200 keV) presented in paper 1.

To demonstrate that the correlation relationship between ion fluxes and θ_{Bx} depends on the ion energy, we perform the cross-correlation analysis for all the CEPPAD ion energy channels. Results are presented in Figure 7. Correlation curves are gray-scale coded according to the ion energy expressed in the gray-scale bar on the right of Figure 7.. It is noted that there are two classes of curves. Three curves for ion energy below 30 keV belong to the first type that show null correlation regardless of the value of the assumed time delay. The rest of the curves for ion energy between 30 keV and 1 MeV belong to the second type, resembling those in Figure 6. They all show a unique peak at about the same assumed lag.
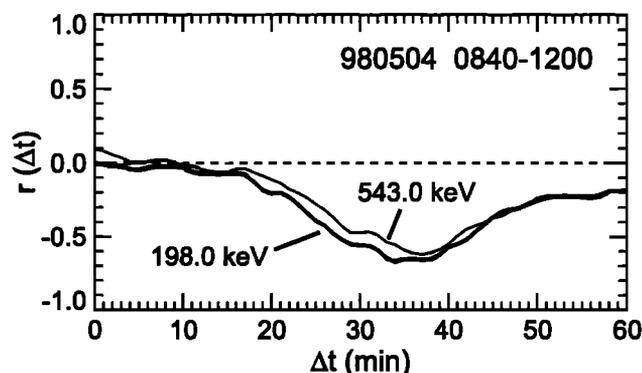
Figure 6. Correlation coefficients calculated at each time lag for θ_{Bx} assumed from 0 to 60 min for 198 keV ions (thick line) and 543 keV ions (thin line).
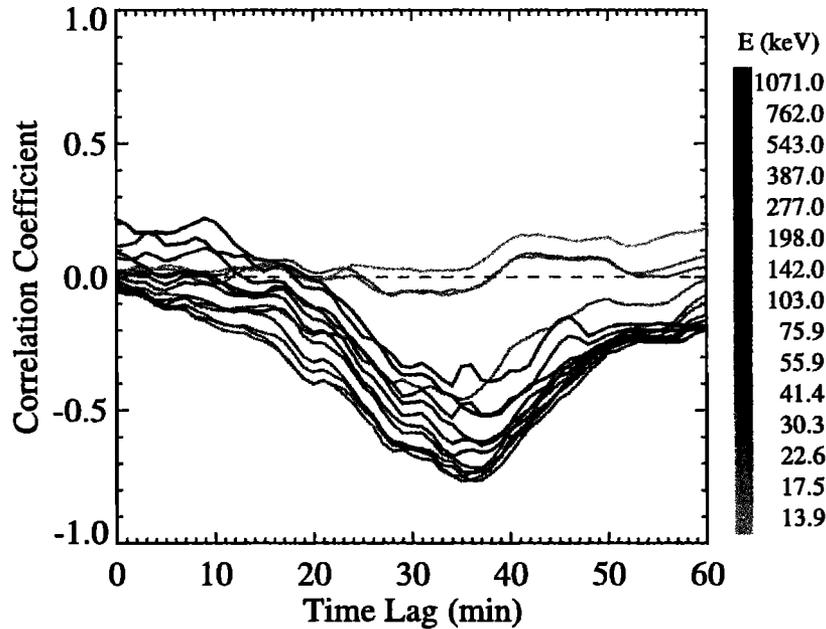
Figure 7. Correlation coefficients for all the CEPPAD ion energy channels that are indicated in the gray-scale bar. Two classes of curves are clearly present. One shows null correlation, and the other shows anticorrelation with only one peak.

The peak correlation coefficient r_o and its corresponding time lag Δt_o are plotted in Figure 8 as a function of ion energy. As shown by the thick line in the top panel, a sharp transition from no correlation to strong anticorrelation appears at the energy channel of 41.4 keV for the CEPPAD ions. This energy threshold for anticorrelation is the same as the spectral break energy of the magnetosheath ion spectrum presented in Figure 3. All the ion fluxes above this energy are anticorrelated with θ_{Bx} with a proper time delay. As shown in the bottom panel, Δt_o for CEPPAD ions above the energy threshold varies within 34-37 min with an average value of 35.5 min. However, it is noted that r_o increases toward 0 as the ion energy gets higher. This may be due to the reduced signal-to-noise ratio in these higher-energy channels. Nevertheless, both the transition energy and the average time delay derived in the CEPPAD energetic ion data are nearly identical to those derived from the CAMMICE ion data (41.1 keV and 36 min) in paper 1.

For comparison, r_o and Δt_o for CAMMICE He$^+$ ions presented in paper 1 are also plotted in Figure 8. The He$^+$ energy in Figure 8 represents the lower bound of the energy range for the total He$^+$ flux integration and He$^+$ curves in this figure would closely reflect the curves for differential energy flux at each energy channel as described in paper 1. Presumably of the ionospheric origin, He$^+$ demonstrates a completely different behavior. Unlike the CAMMICE and CEPPAD energetic ion fluxes, energetic He$^+$ fluxes were quite steady in the magnetosheath interval (see Plate 1 of paper 1). He$^+$ shows inconsistent r_o and Δt_o without any correlation with θ_{Bx} throughout the energy range, ~17-

100 keV. Therefore, CEPPAD energetic ions and CAMMICE He$^+$ would appear to have come from distinct source regions, or at least via different paths if from the same source region.

2.3. Bow Shock Ion Spectrum

During some periods of this magnetosheath event, Interball-Tail was located in the foreshock region upstream from the quasi-parallel bow shock. In particular, Interball was at times very close to, if not exactly at, the source region of magnetosheath energetic ions observed by Polar that we previously proposed (see paper 1 and also *Chang et al.* [1998]). A comparison of Interball and Polar ion spectra can potentially falsify our bow shock source hypothesis and is now the focus of our analysis.

Because the energetic particle data from DOK-2 on Interball were not transmitted to the ground before 1100 UT, we are restricted to the last 1-hour interval of the magnetosheath event for the flux comparison. For ~41 min from 1101 to 1142 UT, Interball was upstream from the quasi-parallel bow shock as illustrated in Figure 9. On the left, Figure 9 shows the xz projections of the bow shock, magnetopause, Interball and Polar orbits, and IMF, and on the right, Figure 9 shows the yz projections of the dayside portion of the bow shock before the terminator, spacecraft orbits, and IMF. This interval is selected for its relatively steady IMF and solar wind conditions so that bow shock geometry and location would remain similar. The bow shock surface is calculated using *Fairfield*'s [1971] model scaled by the solar wind dynamic pressure and the magnetopause sur-

face is calculated from *Shue et al.*'s [1998] model. All the solar wind and IMF parameters used in these models are the average Wind measurements over the interval corrected by the propagation time. As shown in Figure 9, Interball was upstream from the quasi-parallel bow shock (the shaded region on the right) with an average θ_{Bn} of 22° and an average distance of 5.8 R_E along the magnetic field line to the shock. Polar was just outside the model magnetopause in the magnetosheath. We note that Polar was in the undisturbed magnetosheath according to the plasma and magnetic field data; that is, Polar was located farther into the

Figure 8. (top) Peak correlation coefficient r_o and (bottom) the associated time lag Δt_o, both as a function of ion energy E for CEPPAD ion (thick line) and CAMMICE He$^+$ (thin line). A sharp transition from weak correlation to strong anticorrelation appears at the CEPPAD energy channel of 41.4 keV. Δt_o for the CEPPAD ion energy above 41 keV ranges from 34 to 37 min with an average value of 35.5 min.

magnetosheath than that suggested by the model. Both spacecraft were located in the postnoon sector at close longitudes. On the basis of the general plasma flow in the solar wind, magnetosheath, magnetosphere, and ionosphere [e.g., *Spreiter and Stahara*, 1985; *Reiff and Burch*, 1985], we suggest that magnetosheath magnetic field geometry during this interval is similar to those in Figure 11 of paper 1 and Figure 5 of *Chang et al.* [1998], in which cases magnetosheath magnetic field direction is reversed but magnetic field lines and the topology remain similar. Thus Polar is likely to be very well connected to Interball by magnetic field lines.

Using the lag corrected IMF and solar wind measurements from Wind and *Fairfield*'s [1971] bow shock model, we calculated bow shock distance along magnetic field lines and θ_{Bn} associated with Interball for the above 41-min upstream interval. Results are presented in Figure 10. The estimated bow shock distance ranges from 5 to 7 R_E while θ_{Bn} ranges from 11° to 38°. As expected under steady IMF and solar wind conditions, most of the time these two quantities are steady around 6 R_E and 22°. Therefore the average values of bow shock distance (5.8 R_E) and θ_{Bn} (22°) are very good representations of the instantaneous values throughout this upstream interval.

For a direct comparison, energetic ion spectrum from Interball/DOK-2 and magnetosheath ion spectrum from Polar both averaged over 41 min from 1101 to 1142 UT are plotted in Figure 11. During this interval, Polar observed very intense energetic ion fluxes (see, for example, CEPPAD ion fluxes at both energy channels in Figure 5). Once again, the magnetosheath spectrum comprising Hydra, CAMMICE, and CEPPAD measurements shows very good agreement among the individual spectra. Its spectral shape is very similar to the one averaged over the interval more than 3 hours long presented in Figure 3. Both spectra are continuous with a spectral break occurring at the same energy ($\sim$40 keV). The magnetosheath energetic ion spectrum during this upstream event also shows a Maxwellian or exponential distribution for lower-energy energetic ions ($\sim$40-200 keV) and a power law distribution for higher-energy ions ($\sim$200-1000 keV) with a spectral index of 4.1. Therefore this spectrum from $\sim$40 keV to 1 MeV can be described by a κ distribution. Similarly, the energetic ion spectrum observed by Interball/DOK-2 upstream from the bow shock also shows a κ-like distribution. However, these upstream energetic ion fluxes generally do not agree with the magnetosheath fluxes. Disagreement gradually magnifies toward lower ion energy. Nonetheless, above 200 keV, bow shock ion fluxes are close to the magnetosheath values, and their spectral shape is similar to the magnetosheath's. In spite of the disagreement, this result does not rule out the bow shock source of magnetosheath energetic ions as we discuss below.

It is known that the upstream diffuse ion fluxes decrease exponentially along the magnetic field lines away

Figure 9. (left) Projection of the bow shock (BS), magnetopause (MP), and Polar and Interball orbits onto the xz plane. (right) The yz projections of the dayside portion of the bow shock before the terminator, spacecraft orbits, and IMF. The bow shock surface is obtained from *Fairfield*'s [1971] model scaled by the solar wind dynamic pressure, and the magnetopause surface is from *Shue et al.*'s [1998] model. Contours of constant θ_{Bn} shown on the right are calculated using a nearly radial, average IMF $(17.2, 3.8, -3.1)$ nT with $\theta_{Bx} < 20°$.

from the shock [e.g., *Ipavich et al.*, 1981; *Lee*, 1982]. This e-folding distance generally depends on ion energy. Following Figure 7 of *Trattner et al.* [1994] and assuming that e-folding distance scales with solar wind velocity, we can then estimate energetic ion fluxes at the shock. For the simplest assumption we assume that the statistics of *Trattner et al.* [1994] apply to the average solar wind condition and that e-folding distance is inversely proportional to the solar wind speed as suggested by the nature of diffusive transport for ions upstream of quasi-parallel bow shock [*Lee*, 1982]. The resulting e-folding distance for this event is plotted in Figure 12. It ranges between 4 and 6 R_E for the Interball energy channels used in this study. For the average bow shock distance of 5.8 R_E mentioned above, the required correction is $\sim$1.4-1.0 e-foldings, with the lowest-energy ions corrected the most and the highest-energy ions corrected the least.

The corrected spectrum (or the estimated ion spectrum at the bow shock surface) is presented in Figure 13. This bow shock ion spectrum and magnetosheath energetic ion spectrum are nearly indistinguishable. Although the bow shock spectrum ends at $\sim$600 keV (the high-energy limit of useful detection), bow shock energetic ions follow the spectral trend of the magnetosheath spectrum with very high precision. With the bow shock and magnetosheath regions connected by magnetic field lines during this event, this result implies that between the bow shock and magnetosheath energetic ions, one is the source of the other.

As to the acceleration region, we have also included the energetic ion measurements from Wind/3DP in the solar wind $\sim$200 R_E upstream from the bow shock in Figure 13 to check the fluxes of solar energetic particles. According to the bulk speed of the solar wind, the ion spectrum presented here is lagged by 29 min. It is expected that this lag is smaller for energetic ions. However, because energetic ion fluxes were quite steady in the solar wind during the entire magnetosheath event,

Figure 10. Bow shock distance along magnetic field lines (thick line) and θ_{Bn} (thin line) associated with Interball during the interval of 1101-1142 UT.
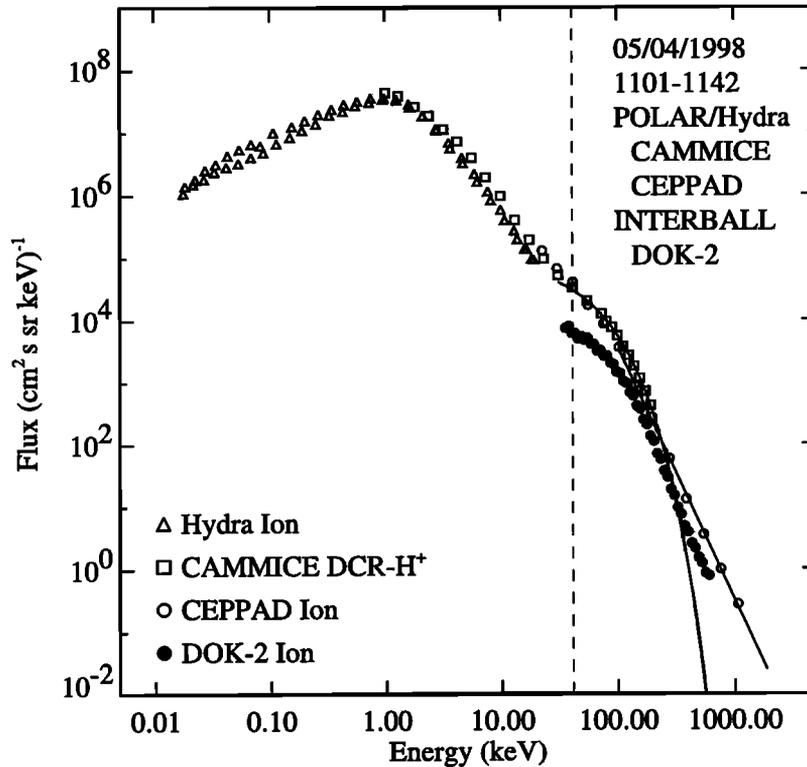
Figure 11. Average magnetosheath ion spectrum from Polar/Hydra, CAMMICE, and CEPPAD and foreshock ion spectrum from Interball/DOK-2 for the interval 1101-1142 UT on May 4, 1998. CAMMICE ions from ~40 to 200 keV are fitted by an exponential function. CEPPAD ions from ~200 keV to 1 MeV are fitted by a power law.

the 3DP ion spectrum presented here is representative. Both the solar energetic ion fluxes and magnetosheath energetic ion fluxes are not correlated as suggested by the results from cross-correlation analysis (results not shown). In addition, from the large disagreement between the ion spectra in the solar wind and at the bow shock, one can immediately draw the conclusion that ion acceleration must take place downstream of the Wind spacecraft.

2.4. Total Energy

In addition to the excellent match between the magnetosheath and bow shock ion spectra shown in Figure 13, the magnetosheath ion spectra observed by Polar during the above upstream event from 1101 to 1142 UT also show characteristics of upstream diffuse ions. As demonstrated in Figure 14, energetic ion spectra for CAMMICE H^+, He^{+2}, and $O^{>+2}$ are organized very well by energy per charge (left panel) not the total energy (right panel). In the left panel of Figure 14, spectra of all three species show a spectral break at ~40 keV e^{-1}. It is noted that the flatness in the He^{+2} and $O^{>+2}$ spectra below ~5 keV e^{-1} reflects poor efficiency of CAMMICE/MICS for these two species at low-energy channels. The spectral break energy is higher than the typical e-folding energy at ~20 keV e^{-1} in the diffuse ion events [e.g., Lee, 1982]. Nonetheless, this is expected because of the large shock Alfvén Mach num-

ber (~7.1) and unusually high solar wind speed (~745 km s^{-1}) in this event [Scholer et al., 1999]. The spectral shapes of these three ion species from 40 keV e^{-1} to the CAMMICE maximum detection energy (~200 keV e^{-1}) are Maxwellian or exponential, consistent with early reports of upstream events in this energy range [e.g., Ipavich et al., 1981].

For the purpose of comparing ion fluxes from Hydra, CEPPAD, and DOK-2 instruments which do not distin-
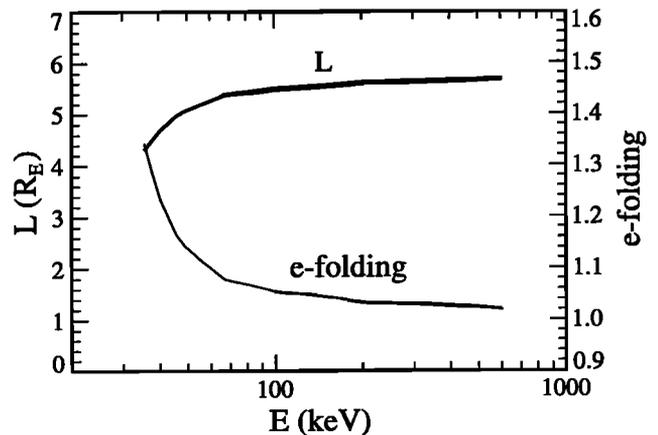
Figure 12. The e-folding distance (thick line) and number of e-foldings (thin line) for correction as a function of ion energy.
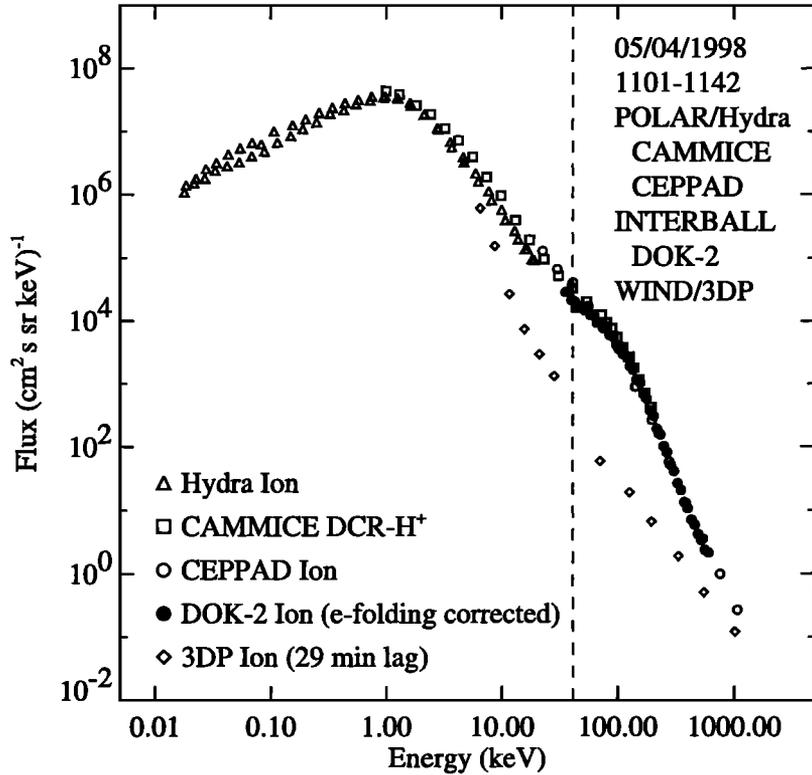
Figure 13. Bow shock ion spectrum from Interball after the e-folding correction and the magnetosheath ion spectrum during the upstream event, 1101-1142 UT. Ion spectrum measured by Wind/3DP in the solar wind is also plotted for reference.

guish ion masses, we have been using total ion measurements from the double coincidence rate (DCR) channel (time-of-flight measurements of all ion species) of the CAMMICE MICS detector. This detector also has a H^+ channel (time-of-flight and energy measurements) that excludes other species. The energy of detection for this channel is from 5.6 to 193.4 keV. H^+ spectrum from this channel measured in the above interval is nearly identical to the DCR-H^+ spectrum presented in Figure 14. This indicates that contributions of other species to the total ion measurements up to 200 keV are negligible. Another estimate of heavy ion contribution to the DCR channel is provided by the direct event (DE) data from MICS. The DE data are detailed measurements from a subset of the ions detected. They are transmitted to the ground and used to verify the correctness of the on board ion sorting algorithms. Examination of the DE data shows that the fluxes of oxygen ions measured during this event are consistent with the fluxes shown in the left panel of Figure 14 and that the DCR response is dominated by H^+ at all energy channels.

There is a question of whether energetic ions from 200 keV to 1 MeV detected by CEPPAD instrument are heavy ions since a 200 keV e^{-1} O^{+6} has a total energy of 1.2 MeV. As shown in the right panel of Figure 14, He^{+2} spectrum from 200 to 400 keV agrees very well with the corresponding CEPPAD ion spectrum, and $O^{>+2}$ (assuming O^{+6}) spectrum shows a trend close to CEPPAD ion spectrum from 600 keV to 1 MeV. At the first

glimpse, the exponential distributions of He^{+2} and O^{+6} seem to comprise the power law spectrum of CEPPAD ions above 200 keV. However, as shown in Figure 14, at lower energies from $\sim$5 to 40 keV, He^{+2} and O^{+6} fluxes can also account for CAMMICE DCR-H^+ and CEPPAD ion fluxes at the corresponding energies. Yet, CAMMICE DCR and CEPPAD ion measurements were most likely H^+ within this energy range because spectra from the CAMMICE H^+ channel, DCR channel, and CEPPAD IPS agree well as described above. Likewise, since we do not know how the CEPPAD IPS detector responds to different ion species at different energies, we cannot argue that CEPPAD detector simply detected He^{+2} and O^{+6} at energy channels above 200 keV for this event. This issue can be resolved with composition measurements above 200 keV e^{-1}. Unfortunately, this is beyond the capability of Polar instruments.

3. Discussion and Conclusion

In our previous work on the CAMMICE energetic (up to 200 keV e^{-1}) ions for this May 4, magnetic storm event, we suggested that energetic ions of solar wind origin (H^+, He^{+2}, $O^{>+2}$) observed at the midlatitude dayside magnetosheath were accelerated at the quasi-parallel region of the bow shock and that those of ionospheric origin (He^+) observed at the same location were accelerated in the magnetosphere. This is supported by

the following evidence with figures within parentheses referring to paper 1 except when noted otherwise.

1. Energy spectra of the above three solar wind ion species are organized very well by energy per charge not the total energy. They all show a spectral break at the same energy at ~40 keV e^{-1}. Their spectral shape within the energy range of 40-200 keV e^{-1} is Maxwellian or exponential, similar to the spectral shape of bow shock diffuse ions [e.g., *Ipavich et al.*, 1981] (Figure 6, also Figure 14 in this paper).

2. Energetic electron and ion composition changed as Polar crossed the magnetopause near the equator and at the midlatitude. Inside the magnetosphere, Polar detected intense energetic electrons, H$^+$, He$^+$, and O$^{<+3}$ and relatively weak He^{+2} and O$^{>+2}$. In the magnetosheath, Polar detected intense energetic H$^+$, He^{+2}, and O$^{>+2}$, nearly no energetic electrons, O$^{<+3}$, and very weak He$^+$ (Plate 1).

3. Intense magnetosheath energetic ions all showed anisotropy toward the magnetopause and a strong tailward flow away from the bow shock (Figure 9).

4. The three magnetosheath energetic ion fluxes of solar wind origin showed large temporal variations as high as 2 orders of magnitude. Fluxes at energies above

the energy of the spectral break (~40 keV e^{-1}) are anticorrelated with the IMF cone angle with a time delay consistent with the solar wind propagation time and the acceleration time for shock acceleration. This correlation relationship disappeared for ion fluxes at energies below this energy threshold. On the contrary, He$^+$ fluxes were relatively steady throughout the entire magnetosheath interval. They are not correlated with the cone angle at all energies (Plates 1 and 2, Figures 7 and 8).

5. When the intensities of the above three solar wind ion species were high, Polar was connected to the quasi-parallel, dayside region of the bow shock by magnetic field lines. When their intensities were low, Polar was disconnected from the above region (Figure 11).

6. The ion spectrum observed at the quasi-parallel bow shock by Interball/DOK-2 agreed very well with the magnetosheath ion spectra simultaneously observed by Polar/CAMMICE and CEPPAD as demonstrated in Figure 13.

A simple explanation for the above results is that the intense magnetosheath energetic ions (up to 200 keV e^{-1}) of solar wind origin are accelerated at the dayside quasi-parallel bow shock by the Fermi mechanism [e.g.,
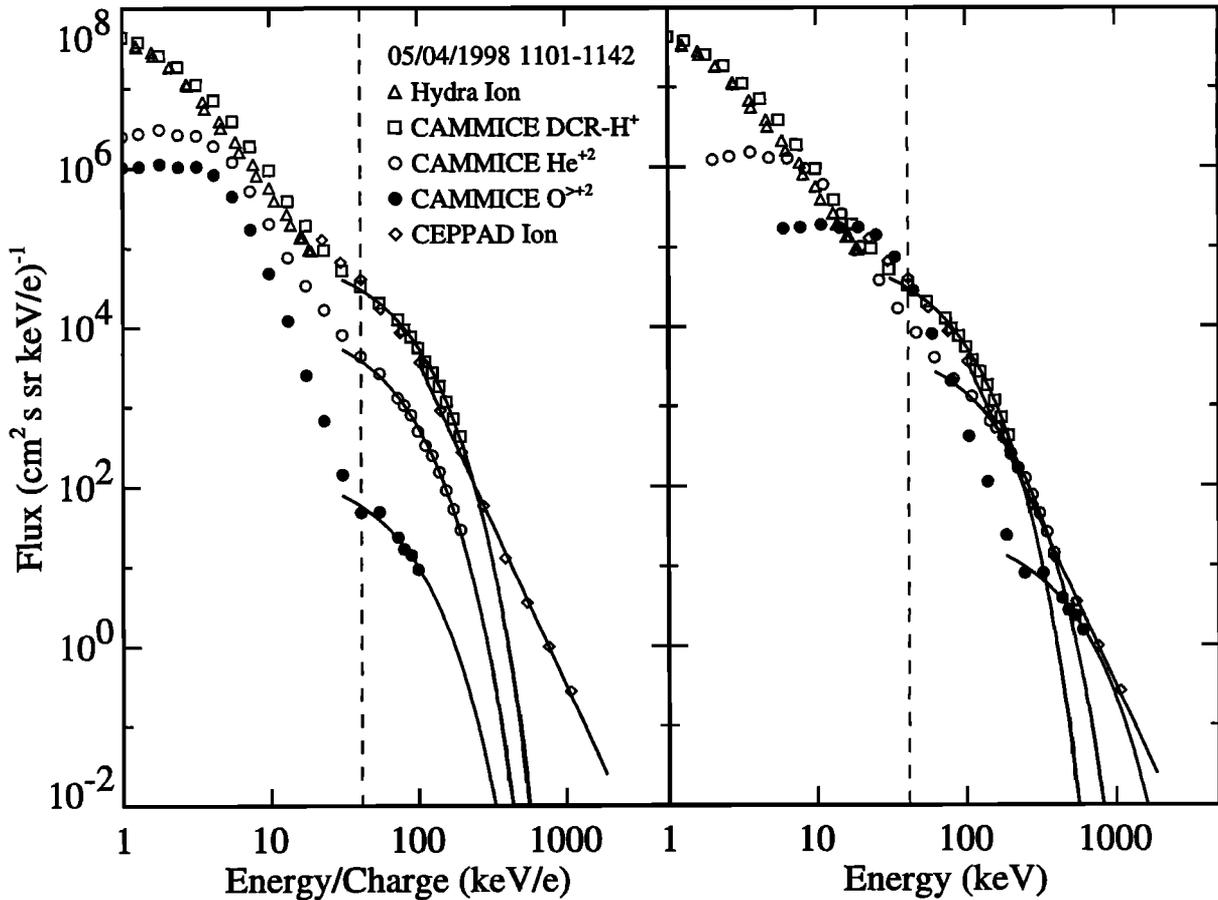
Figure 14. Magnetosheath ion spectrum extracted from Figure 11 with the addition of the CAMMICE/He^{+2} and O$^{>+2}$ (assuming O^{+6}) spectra in (left) energy per charge and (right) total energy during the upstream event, 1101-1142 UT. All the curves represent exponential distributions.

Scholer et al., 1980; *Lee*, 1982; *Ellison*, 1985; *Fuselier et al.*, 1991]. Intensities of these ions change as the IMF orientation changes so that Polar is magnetically connected or disconnected to this shock region. Solar wind ions accelerated at the quasi-parallel shock are directly transported along field lines to the midlatitude magnetosheath when two regions are connected (see Figure 11 of paper 1). The nearly steady, weak He^+ ions are mostly from the magnetospheric leakage [e.g., *Croley et al.*, 1986; *Sibeck et al.*, 1987; *Kudela et al.*, 1992; *Christon et al.*, 1994]. This leakage process invokes diffusive transport and finite larmor radius effect across the equatorial magnetopause. The intensity of the leakage is more or less related to the substorm activities not the bow shock magnetic geometry. Because Polar was on field lines that threaded through the equatorial magnetosheath near the magnetopause all the time regardless of the IMF orientation, He^+, leaking from the magnetosphere, could reach Polar along field lines persistently. Since He^+ is less than 1% of the total energetic ion population, magnetospheric leakage can only account for a small fraction of the magnetosheath energetic ions detected by the CAMMICE instrument.

Other possible explanations for the Polar observations of magnetosheath energetic ions include injection of magnetospheric energetic ions and local acceleration in the cusp that recently appear in the literature. Several groups using single-particle simulations have shown that energetic ions trapped on closed field lines occasionally can escape into the cusp region especially during substorms [*Delcourt and Sauvaud*, 1999; *Blake*, 1999; *Spence et al.*, 1999]. These ions can subsequently leak into the magnetosheath along the reconnected field lines [e.g., *Scholer et al.*, 1981]. However, as we had reported in paper 1, Polar was on magnetosheath field lines nearly all the time connecting to the solar wind, not open magnetospheric regions (cusp, mantle, lobe, etc.) during this event. Therefore the path for such a leakage process was not present in this Polar orbit. Accordingly, cusp energetic ions whether they were energetic ions escaping from ring current/plasma sheet or solar wind ions locally accelerated in the cusp [*Chen and Fritz*, 1999] would not escape into the magnetosheath to be detected by Polar. Furthermore, we note that Polar never traversed through the cusp according to the electron data and that there is no direct evidence of particle acceleration in the cusp for this event. Contrary to *Chen and Fritz*'s [1999] proposal of cusp energetic ions being the source of magnetosheath energetic ions, we suggested in paper 1 that these bow shock accelerated magnetosheath energetic ions (up to 200 keV e^{-1}) are at times a plausible source of cusp energetic ions [*Chang et al.*, 2000].

The detection of MeV magnetosheath ions by the Polar CEPPAD instrument raises the question about their origin. For reasons described above, the above two ac-

celeration and transport processes, namely, magnetospheric ion injection [e.g., *Delcourt and Sauvaud*, 1999] and cusp acceleration [*Chen and Fritz*, 1999], are implausibly the cause. Since the magnetosphere is full of MeV ions, magnetospheric leakage can be a candidate for those CEPPAD ions [*Sibeck et al.*, 1987]. However, there is some evidence against this argument.

1. CEPPAD ion spectrum below 200 keV agrees very well with CAMMICE ion spectrum, and CEPPAD ions above 200 keV simply extend the energetic ion spectrum to form a power law tail. The entire energetic ion spectrum is continuous. This may indicate a unique source region since bow shock ion spectra produced by the Fermi process and originating from the magnetospheric leakage are quite different [*Möbius et al.*, 1986]. Because the lower-energy portion of the energetic ion spectrum comes from the shock and very few energetic (up to 200 keV e^{-1}) ions come from the magnetosphere, it is very possible that the higher-energy portion of the spectrum also comes from the shock, not the magnetosphere.

2. The leakage process has difficulty explaining the anticorrelation between the IMF cone angle and the magnetosheath energetic ion fluxes at each CEPPAD energy channel from 40 keV to 1 MeV. Since Polar was at midlatitude magnetosheath on magnetic field lines threading the equatorial magnetosheath region where ions escaping from the magnetosphere would immediately reach, a part of these ions would readily reach Polar along field lines. Because magnetospheric leakage continuously occurs at the magnetopause [*Sibeck et al.*, 1987], Polar would observe magnetospheric ions persistently during this event. These ions are expected to show no correlation with the IMF cone angle just like those He^+ ions detected by CAMMICE. This is not the case for the 40-1000 keV ions detected by the CEPPAD instrument, which behave very similarly to the 40-200 keV e^{-1} H^+, He^{+2}, and $O^{>+2}$ ions detected by CAMMICE.

The above two points, however, suggest that the source of MeV magnetosheath ions is the bow shock diffuse ions. In addition, results of cross-correlation analysis for the CEPPAD energetic ion flux and IMF cone angle show features identical to those for the CAMMICE ion flux of solar wind origin in our previous study. For example, the correlation coefficient shows a sharp transition from no correlation at $\sim$20 keV to strong anticorrelation at $\sim$40 keV and beyond. This energy threshold for the anticorrelation is identical to the energy at the spectral break of magnetosheath ion spectrum. The time delay for best anticorrelation at each ion energy from 40 keV to 1 MeV is nearly the same at $\sim$36 min. This lag is consistent with the estimated solar wind propagation time $\sim$29 min during this event (see paper 1) plus the growth time for bow shock diffuse ions $\sim$10 min [e.g., *Scholer et al.*, 1980; *Mitchell and*

Roelof, 1983]. This single acceleration time, $\sim$7 min, for ions from 40 keV to 1 MeV might appear to be an implausible result of a simple Fermi process from a thermal distribution. There are three possible explanations that are described in detail later.

In addition to the above evidence, an important piece of evidence for the bow shock source is demonstrated in Figure 13. Magnetosheath energetic ion spectrum and simultaneously observed bow shock ion spectrum agree very well up to $\sim$600 keV, and the spectral trend of the bow shock ions also agrees very well with the magnetosheath spectrum above this energy. This flux comparison has significance because Interball and Polar are arguably connected by the magnetic field line during this upstream interval. Energetic ions at the quasi-parallel bow shock region that is magnetically connected to Interball can simply follow the field line and reach the Polar's location in the magnetosheath. Using Liouville's theorem, the distribution function is conserved along particle's trajectory provided there are no collisions. As long as particle energy is the same at the two regions, flux remains the same. However, particle spectra were often compared in two different regions in the literature. Without establishing the link between two regions, the Geotail and Polar ion flux comparison by *Chen and Fritz* [1999] for this storm event can be wrong. In that example, Geotail was located in the duskside and nightside of the equatorial magnetosheath, and Polar was at the midlatitude dayside magnetosheath near local noon. Under the solar wind and IMF conditions for this event, the above two regions are very likely on quite different magnetic field lines and streamlines. Therefore Geotail data convey no information concerning the Polar observations of magnetosheath energetic ions.

The fact that bow shock and magnetosheath ion spectra match so well and MeV magnetosheath ion flux is anticorrelated with the IMF cone angle implies the presence of MeV ions at the shock with the same flux level as the magnetosheath ions. Diffuse ions with energies up to 1 MeV are all accelerated at the shock with the same growth time of $\sim$7 min. As pointed out before, this unique acceleration time may argue against the Fermi mechanism, and 7 min seems too short to accelerate ions to MeV. However, three factors may possibly explain this unique acceleration time. First, seed population: As shown in Figure 13, energetic ion fluxes measured by Wind/3DP at about L1 get closer to the bow shock and magnetosheath values as ion energy increases. The intensity and spectral shape for the energetic ions persisted in the solar wind throughout the whole interval from 0840 to 1200 UT, regardless of the IMF orientation. This indicates that these ions are not bow shock diffuse ions escaping upstream. Otherwise, Wind would have detected higher/lower energetic ion fluxes when the IMF cone angle was small/large and Wind was connected/disconnected to the quasi-parallel

bow shock during this event. In fact, these energetic ions in the solar wind can become the seed population for the Fermi process, and accelerating these ions to MeV requires much shorter time than accelerating keV solar wind ions to MeV [e.g., *Ellison*, 1987]. Although, in general, magnetospheric leakage can also be another source of the seed population [e.g., *Sarris et al.*, 1976], results from plasma composition measurements and the cross-correlation analysis demonstrated in our previous and present work argue against this possibility. Second, acceleration efficiency: The shock Alfvén Mach number during this event was large, and Fermi acceleration became much more efficient [*Scholer et al.*, 1999]. Third, heavy ions: It is well known that heavy ions in the solar wind can be accelerated to $\sim$150 keV e^{-1} through the Fermi process at the quasi-parallel bow shock [e.g., *Ipavich et al.*, 1981; *Galvin et al.*, 1984; *Desai et al.*, 2000]. Therefore high charge state heavy ions can contribute energy exceeding 1 MeV. As shown in Figure 14, He^{+2} and $O^{>+2}$ ions observed by CAMMICE can possibly comprise the CEPPAD energetic ion spectrum above 200 keV. It would take much less time accelerating O^{+6} ions to 200 keV e^{-1} or 1.2 MeV than accelerating H^+ ions to 1 MeV.

In reality, solar wind energetic ions as a seed population and bow shock accelerated heavy ions both might contribute to the MeV magnetosheath ions observed by CEPPAD. Because of the lack of composition measurements above 200 keV e^{-1} in the Polar instruments, we cannot discern the heavy ion contribution. However, CAMMICE direct event data suggest that heavy ion ($M > 20$) contribution is insignificant in the DCR channel during the upstream event, 1101-1142 UT. If the contribution from the solar energetic ion source to MeV ions dominates, the energy limit imposed by the boundary condition in the Fermi model of shock acceleration may need to be modified. It is generally assumed that the Fermi process can produce ion energy up to $\sim$150 keV e^{-1} [e.g., *Ipavich et al.*, 1981; *Lee*, 1982; *Desai et al.*, 2000]. As shown in this event, ions are accelerated to 200 keV e^{-1} and beyond at the shock. In addition, recent Wind statistics shows more than 30% of upstream events demonstrating a power law spectrum extending above 150 keV e^{-1} with ion composition similar to that in the solar wind [*Desai et al.*, 2000]. These results suggest that the so-called "Fermi limit" in the shock literature may require modification. As noted, Fermi mechanism by itself for a plane, infinite shock produces a power law distribution [*Lee*, 1982]. A loss mechanism, such as the upstream escape boundary, cross-field diffusion, disconnection of field lines from the shock, or a combination of these is often included in the Fermi model to reproduce the observed exponential distribution from the ISEE spacecraft [e.g., *Lee*, 1982]. For this upstream event, more realistic boundary conditions in the form of realistic seed population have to be con-

sidered in the Fermi shock model to reproduce the observed bow shock ion spectrum.

4. Summary

During the May 4, 1998, storm event, Wind, Interball-Tail, and Polar observed plasmas of great intensity. In our previous study [*Chang et al.*, 2000] (paper 1), magnetosheath ions were examined up to the CAMMICE maximum detection energy at $\sim$200 keV e^{-1}. It was concluded that energetic ions of solar wind origin came from the quasi-parallel bow shock and that those of ionospheric origin came from the magnetosphere. In this study we extend the magnetosheath ion energy to 1 MeV detected by the CEPPAD instrument, and we provide new evidence for the bow shock source by comparing ion fluxes simultaneously measured in the magnetosheath and at the bow shock source region. Ion spectrum observed by Polar in the midlatitude dayside magnetosheath is continuous and demonstrates a κ-like distribution in the energy range from 40 keV to 1 MeV, which includes a power law tail above 200 keV. Cross-correlation analysis of magnetosheath energetic ions observed by CEPPAD and IMF cone angle shows results identical to those in our previous analysis for lower-energy ions observed by CAMMICE. Magnetosheath ion fluxes above 40 keV are strongly anticorrelated with the cone angle with a time delay consistent with the solar wind propagation time and growth time of upstream diffuse ions. Below this energy, anticorrelation disappears. This energy threshold for the anticorrelation relationship is the same as the energy of the spectral break in the ion spectrum. Among various acceleration and transport mechanisms, such as bow shock acceleration, magnetospheric leakage, substorm injections, and local acceleration in the cusp, our previous and present analyses of the plasma and field data from the above three spacecraft strongly favor the bow shock acceleration for ions of solar wind origin. A causal relationship between bow shock accelerated ions and magnetosheath energetic ions is further demonstrated as bow shock energetic ion spectrum from Interball matches extraordinarily well the magnetosheath energetic ion spectrum from Polar. The e-folding energy of the diffuse ion spectra (40 keV e^{-1}) is higher than the typical value of $\sim$20 keV e^{-1} as expected for large-shock Alfvén Mach number and very high solar wind speed in this event [*Scholer et al.*, 1999]. The acceleration region is at the quasi-parallel bow shock although seed population and heavy ion contribution have yet to be determined. This shock acceleration event producing ion energy above 200 keV e^{-1} is not unique. As demonstrated in the recent Wind statistics, more than 30% of upstream events show a power law spectrum extending above 150 keV e^{-1} [*Desai et al.*, 2000]. This study and the Wind statistics suggest that the so-called "Fermi limit" may require modification. The bow shock source of magnetosheath energetic ions for this event strongly supports the bow shock model of cusp energetic ions [*Chang et al.*, 1998] and is inconsistent with the model of local acceleration in the cusp [*Chen et al.*, 1998].

References

Blake, J. B., Comment on "Cusp: A new acceleration region of the magnetosphere" by J. Chen et al., *Czech. J. Phys.*, *49*, 675, 1999.

Blake, J. B., et al., CEPPAD comprehensive energetic particle and pitch angle distribution experiment on Polar, *Space Sci. Rev.*, *71*, 531, 1995.

Bonifazi, C., and G. Moreno, Reflected and diffuse ions backstreaming from the Earth's bow shock, *J. Geophys. Res.*, *86*, 4405, 1981.

Chang, S.-W., et al., Cusp energetic ions: A bow shock source, *Geophys. Res. Lett.*, *25*, 3729, 1998.

Chang, S.-W., J. D. Scudder, J. F. Fennell, R. Friedel, R. P. Lepping, C. T. Russell, K. J. Trattner, S. A. Fuselier, W. K. Peterson, and H. E. Spence, Energetic magnetosheath ions connected to the Earth's bow shock: Possible source of cusp energetic ions, *J. Geophys. Res.*, *105*, 5471, 2000.

Chen, J., and T. A. Fritz, May 4, 1998 storm: Observations of energetic ion composition by Polar, *Geophys. Res. Lett.*, *26*, 2921, 1999.

Chen, J., T. A. Fritz, R. B. Sheldon, H. E. Spence, W. N. Spjeldvik, J. F. Fennell, S. Livi, C. T. Russell, J. S. Pickett, and D. A. Gurnett, Cusp energetic particle events: Implications for a major acceleration region of the magnetosphere, *J. Geophys. Res.*, *103*, 69, 1998.

Christon, S. P., D. C. Hamilton, G. Gloeckler, T. E. Eastman, and F. M. Ipavich, High charge state carbon and oxygen ions in Earth's equatorial quasi-trapping region, *J. Geophys. Res.*, *99*, 13,465, 1994.

Croley, D. R., Jr., J. F. Fennell, and B. G. Ledley, Observation of reconnection phenomena at synchronous orbit, *J. Geophys. Res.*, *91*, 4321, 1986.

Delcourt, D. C., and J.-A. Sauvaud, Populating of the cusp and boundary layers by energetic (hundreds of keV) equatorial particles, *J. Geophys. Res.*, *104*, 22,635, 1999.

Desai, M. I., G. M. Mason, J. R. Dwyer, J. E. Mazur, T. T. von Rosenvinge, and R. P. Lepping, Characteristics of energetic ($\gtrsim$ 30 keV/nucleon) ions observed by the Wind/STEP instrument upstream of the Earth's bow shock, *J. Geophys. Res.*, *105*, 61, 2000.

Ellison, D. C., Shock acceleration of diffuse ions at the Earth's bow shock: Acceleration efficiency and A/Z enhancement, *J. Geophys. Res.*, *90*, 29, 1985.

Ellison, D. C., Comment on "Magnetospheric origin of en-

ergetic ($E \geq 50$ keV) ions upstream of the bow shock: The October 31, 1977, event" by G. C. Anagnostopoulos et al., *J. Geophys. Res., 92,* 12,458, 1987.

Fairfield, D. H., Average and unusual locations of the Earth's magnetopause and bow shock, *J. Geophys. Res., 76,* 6700, 1971.

Fuselier, S. A., D. M. Klumpar, and E. G. Shelley, On the origins of energetic ions in the Earth's dayside magnetosheath, *J. Geophys. Res., 96,* 47, 1991.

Galvin, A. B., F. M. Ipavich, G. Gloeckler, D. Hovestadt, B. Klecker, and M. Scholer, Solar wind ionization temperatures inferred from the charge state composition of diffuse particle events, *J. Geophys. Res., 89,* 2655, 1984.

Gosling, J. T., J. R. Asbridge, S. J. Bame, G. Paschmann, and N. Sckopke, Observations of two distinct populations of bow shock ions in the upstream solar wind, *Geophys. Res. Lett., 5,* 957, 1978.

Ipavich, F. M., A. B. Galvin, G. Gloeckler, M. Scholer, and D. Hovestadt, A statistical survey of ions observed upstream of the Earth's bow shock: Energy spectra, composition, and spatial variation, *J. Geophys. Res., 86,* 4337, 1981.

Kudela, K., D. G. Sibeck, M. Slivka, S. Fischer, V. N. Lutsenko, and D. Venkatesan, Energetic electrons and ions in the magnetosheath at low and medium latitudes: Prognoz 10 data, *J. Geophys. Res., 97,* 14,849, 1992.

Kudela, K., M. Slivka, J. Rojko, and V. N. Lutsenko, The apparatus DOK-2 (Project Interball): Output data structure and modes of operation, *UEF 01-95,* pp.18, Inst. of Exp. Phys., Kosice, Slovakia, March 1995.

Lee, M. A., Coupled hydromagnetic wave excitation and ion acceleration upstream of the Earth's bow shock, *J. Geophys. Res., 87,* 5063, 1982.

Lepping, R. P., et al., The Wind magnetic field investigation, *Space Sci. Rev., 71,* 207, 1995.

Lin, R. P., et al., A three-dimensional plasma and energetic particle investigation for the Wind spacecraft, *Space Sci. Rev., 71,* 125, 1995.

Lutsenko, V. N., J. Rojko, K. Kudela, T. V. Gretschko, J. Balaz, J. Matisin, E. T. Sarris, K. Kalaitzides, and N. Paschalidis, Energetic Particle Experiment DOK-2 (Interball Project), in *Interball Mission and Payload,* Cent. Natl. d'Etud. Spatiales, Toulouse, France, pp.249-255, 1995.

Mitchell, D. G., and E. C. Roelof, Dependence of 50-keV upstream ion events at IMP 7&8 upon magnetic field bow shock geometry, *J. Geophys. Res., 88,* 5623, 1983.

Möbius, E., D. Hovestadt, B. Klecker, M. Scholer, F. M. Ipavich, C. W. Carlson, and R. P. Lin, A burst of energetic O^+ ions during a upstream particle event, *Geophys. Res. Lett., 13,* 1372, 1986.

Ogilvie, K. W., et al., SWE, A comprehensive plasma instrument for the Wind spacecraft, *Space Sci. Rev., 71,* 55, 1995.

Reiff, P. H., and J. L. Burch, IMF B_y-dependent plasma flow and Birkeland currents in the dayside magnetosphere, 2, A global model for northward and southward IMF, *J. Geophys. Res., 90,* 1595, 1985.

Reiff, P. H., T. W. Hill, and J. L. Burch, Solar wind injection at the dayside magnetospheric cusp, *J. Geophys. Res., 82,* 479, 1977.

Russell, C. T., R. C. Snare, J. D. Means, D. Pierce, D. Dearborn, M. Larson, G. Barr, and G. Le, The GGS/Polar magnetic field investigation, *Space Sci. Rev., 71,* 563, 1995.

Sarris, E. T., S. M. Krimigis, and T. P. Armstrong, Observations of magnetospheric bursts of high-energy protons and electrons at ~35 R_E with Imp 7, *J. Geophys. Res., 81,* 2341, 1976.

Scholer, M., F. M. Ipavich, G. Gloeckler, and D. Hovestadt, Conditions for acceleration of energetic ions ≥ 30 keV associated with the Earth's bow shock, *J. Geophys. Res., 85,* 4602, 1980.

Scholer, M., F. M. Ipavich, G. Gloeckler, D. Hovestadt, and B. Klecker, Leakage of magnetospheric ions into the magnetosheath along reconnected field lines at the dayside magnetopause, *J. Geophys. Res., 86,* 1299, 1981.

Scholer, M., H. Kucharek, and K.-H. Trattner, Injection and acceleration of H^+ and He^{2+} at Earth's bow shock, *Ann. Geophys., 17,* 583, 1999.

Scudder, J. D., et al., Hydra: A 3-dimensional electron and ion hot plasma instrument for the Polar spacecraft of the GGS mission, *Space Sci. Rev., 71,* 459, 1995.

Shue, J.-H., et al., Magnetopause location under extreme solar wind conditions, *J. Geophys. Res., 103,* 17,691, 1998.

Sibeck, D. G., R. W. McEntire, A. T. Y. Lui, R. E. Lopez, A. M. Krimigis, R. B. Decker, L. J. Zanetti, and T. A. Potemra, Energetic magnetospheric ions at the dayside magnetopause: Leakage or merging?, *J. Geophys. Res., 92,* 12,097, 1987.

Speiser, T. W., D. J. Williams, and H. A. Garcia, Magnetospherically trapped ions as a source of magnetosheath energetic ions, *J. Geophys. Res., 86,* 723, 1981.

Spence, H. E., T. A. Fritz, J. D. Sullivan, J. F. Fennell, X. Li, M. Grande, and C. Perry, Multispacecraft studies of high-magnetic-latitude velocity-dispersed particle signatures, *Eos Trans. AGU, 80*(46), Fall Meet. Suppl., F890, 1999.

Spreiter, J. R., and S. S. Stahara, Magnetohydrodynamic and gasdynamic theories for planetary bow waves, in *Collisionless Shocks in the Heliosphere: Reviews of Current Research, Geophys. Monogr. Ser.,* vol. 35, edited by B. T. Tsurutani and R. G. Stone, p. 85, AGU, Washington, D. C., 1985.

Trattner, K. J., E. Möbius, M. Scholer, B. Klecker, M. Hilchenbach, and H. Lühr, Statistical analysis of diffuse ion events upstream of the Earth's bow shock, *J. Geophys. Res., 99,* 13,389, 1994.

Vasyliunas, V. M., A survey of low-energy electrons in the evening sector of the magnetosphere with OGO 1 and OGO 3, *J. Geophys. Res., 73,* 2839, 1968.

Wilken, B., W. Weiss, D. Hall, M. Grande, F. Soraas, and J. F. Fennell, Magnetospheric ion composition spectrometer onboard the CRRES spacecraft, *J. Spacecr. Rockets, 29,* 585, 1992.

S.-W. Chang, Center for Space Plasma and Aeronomic Research, University of Alabama in Huntsville, Huntsville, AL 35899. (changs@cspar.uah.edu)

J. F. Fennell, The Aerospace Corporation, Mail Stop M2-259, Los Angeles, CA 90009.

K. Kudela, Institute of Experimental Physics, Slovak Academy Sciences, Kosice 04353, Slovakia.

R. P. Lepping, NASA Goddard Space Flight Center, Code 696.0, Greenbelt, MD 20771.

R. P. Lin, Space Sciences Laboratory, University of California, Berkeley, CA 94720.

C. T. Russell, Institute of Geophysics and Planetary Physics, University of California, Los Angeles, CA 90095.

J. D. Scudder, Department of Physics and Astronomy, University of Iowa, Iowa City, IA 52242.

H. E. Spence, Boston University, Department of Astronomy and Space Physics, 725 Commonwealth Ave., Boston, MA 02215.